

Published in final edited form as:

*Cell Rep.* 2014 November 6; 9(3): 1023–1033. doi:10.1016/j.celrep.2014.09.037.

## Sorting Nexin 27 Regulates A $\beta$ Production through Modulating $\gamma$ -secretase Activity

Xin Wang<sup>1,2</sup>, Timothy Huang<sup>2</sup>, Yingjun Zhao<sup>2</sup>, Qiuyang Zheng<sup>1,2</sup>, Robert C. Thompson<sup>2</sup>, Guojun Bu<sup>1</sup>, Yun-wu Zhang<sup>1,2</sup>, Wanjin Hong<sup>3,4</sup>, and Huaxi Xu<sup>1,2,\*</sup>

<sup>1</sup>Fujian Provincial Key Laboratory of Neurodegenerative Disease and Aging Research, Institute of Neuroscience, Medical College, Xiamen University, Xiamen 361005, China

<sup>2</sup>Degenerative Disease Research Program, Center for Neuroscience, Aging, and Stem Cell Research, Sanford-Burnham Medical Research Institute, La Jolla, CA 92037, USA

<sup>3</sup>Institute for Biomedical Research, School of Pharmaceutical Sciences, Xiamen University, Xiamen 361005, China

<sup>4</sup>Institute of Molecular and Cell Biology, 61 Biopolis Drive, Singapore 138673, Singapore

### SUMMARY

Patients with Down syndrome (DS) invariably develop Alzheimer's disease (AD) pathology in their 40s. We have recently found that overexpression of a chromosome 21-encoded microRNA-155 results in decreased levels of the membrane trafficking component, SNX27, diminishing glutamate receptor recycling and thereby impairing synaptic functions in DS. Here we report a function of SNX27 in regulating A $\beta$  generation by modulating  $\gamma$ -secretase activity. Downregulation of SNX27 using RNA interference increased A $\beta$  production, whereas overexpression of full-length SNX27 but not SNX27 PDZ reversed the RNAi-mediated A $\beta$  elevation. Moreover, genetic deletion of *Snx27* promoted A $\beta$  production and neuronal loss, whereas overexpression of SNX27 using an AAV vector reduced hippocampal A $\beta$  levels in a transgenic AD mouse model. SNX27 associates with the  $\gamma$ -secretase complex subunit presenilin 1; this interaction dissociates the  $\gamma$ -secretase complex, thus decreasing its proteolytic activity. Our study establishes a molecular mechanism for A $\beta$ -dependent pathogenesis in both DS and AD.

### INTRODUCTION

Down Syndrome (DS) or trisomy 21 is a congenital disorder manifesting defects in multiple organs and causing developmental delay and learning disabilities. DS patients have an extra copy of chromosome 21, leading to an over-dosage of gene products and non-coding RNAs encoded by this chromosome, including the  $\beta$ -amyloid precursor protein (APP). APP can be

© 2014 The Authors. Published by Elsevier Inc.

\*To whom correspondence may be addressed. xuh@sanfordburnham.org.

**Publisher's Disclaimer:** This is a PDF file of an unedited manuscript that has been accepted for publication. As a service to our customers we are providing this early version of the manuscript. The manuscript will undergo copyediting, typesetting, and review of the resulting proof before it is published in its final citable form. Please note that during the production process errors may be discovered which could affect the content, and all legal disclaimers that apply to the journal pertain.

proteolytically cleaved by  $\beta$ -secretase (BACE1) and presenilin 1 (PS1)/ $\gamma$ -secretase to generate neurotoxic  $\beta$ -amyloid (A $\beta$ ) peptides. Overproduction/accumulation of A $\beta$  in the brain contributes to DS pathogenesis and is a causative factor in Alzheimer's disease (AD) pathogenesis. Virtually all DS patients develop AD-like neuropathology by the age of 40, including extracellular neuritic/amyloid plaques comprising A $\beta$  peptides of varying sizes, intracellular neurofibrillary tangles, synaptic dysfunction, and neurodegeneration in vulnerable brain regions. While the extra-copy of APP on chromosome 21 is thought to contribute to the AD-like pathology in DS patients, the detailed molecular mechanisms by which trisomy 21 results in AD-like neuropathology remain largely unclear. The majority of early onset familial AD cases are associated with mutations in *PS1*, *PS2* and *APP* genes – all of which resulting in A $\beta$  over-production (Bertram et al., 2010; Shen, 2013). Multiple lines of evidence suggest that over-production/aggregation of A $\beta$  in the brain is the primary cause of AD pathogenesis. Current A $\beta$ -directed therapeutic strategies mainly target  $\beta$ -secretase (BACE1) or the  $\gamma$ -secretase complex. The  $\gamma$ -secretase complex itself is a multimeric aspartyl protease composed of at least four subunits: PS1 (or PS2), Nicastrin, Aph-1 and Pen-2 (De Strooper and Annaert, 2010; Goutte et al., 2002; Hasegawa et al., 2004; Kimberly et al., 2003; Sherrington et al., 1995; Yu et al., 2000). Recently, some  $\gamma$ -secretase interacting components have been identified, which modulate  $\gamma$ -secretase activity, including CD147 (Zhou et al., 2005), TMP21 (Chen et al., 2006), phospholipase D1 (Cai et al., 2006), Rer1p (Spasic et al., 2007), Arc (Wu et al., 2011), and  $\beta$ -arrestin1/2 (Liu et al., 2013; Thathiah et al., 2013). However, the molecular mechanism of  $\gamma$ -secretase activity regulation is still largely unknown and more work is needed to identify novel  $\gamma$ -secretase binding partners and define the molecular and cellular mechanisms involved in regulating  $\gamma$ -secretase activity.

Sorting nexins (SNXs) belong to a large family of proteins containing a conserved PX domain. Many members of this family have been shown to regulate protein sorting in early endosomes. Although 33 mammalian SNXs and 10 yeast SNXs have been currently identified many of the SNX proteins remain uncharacterized with respect to their function (Cullen, 2008). Interestingly, several SNXs have been found to regulate APP trafficking and cleavage, including SNX12, SNX17 and SNX33 (Lee et al., 2008; Schobel et al., 2008; Zhao et al., 2012). SNX27 was initially identified in rats as a product generated from alternative splicing of the *Mrt1* (methamphetamine responsive transcript 1) gene. SNX27 comprises two variants, SNX27a and SNX27b. SNX27a is expressed constitutively in the brain and testis, whereas SNX27b is induced in the brain following methamphetamine treatment (Kajii et al., 2003). As a PX domain protein, SNX27 co-localizes with EEA1 in early endosomes and transferrin receptors in recycling endosomes (Cai et al., 2011). In addition, SNX27 exclusively contains a PDZ domain which is not found in other PX domain proteins. PDZ domains are protein-protein interaction domains that are often found in the postsynaptic density of neuronal excitatory synapses. Our previous studies showed that SNX27 deficiency contributes to the synaptic and cognitive deficits in DS patients, and over-expression of SNX27 in a Ts65Dn DS mouse model rescues associated cognitive and synaptic impairments (Wang et al., 2013). Although the mechanism underlying SNX27 deficiency-induced synaptic dysfunction has been linked to the dysregulation of glutamate receptor trafficking (Loo et al., 2014; Wang et al., 2013b), whether SNX27 deficiency

contributes to other aspects of DS neuropathology, especially amyloid burden, still remains unknown.

Here, we identified SNX27 as a novel  $\gamma$ -secretase interaction partner and a regulator of  $\gamma$ -secretase activity. We demonstrated that depletion of SNX27 results in increased  $\gamma$ -secretase activity and A $\beta$  production, and over-expression of the SNX27 protein decreases A $\beta$  generation in AD transgenic mice by inhibiting  $\gamma$ -secretase activity. Identification of SNX27's role in modulating  $\gamma$ -secretase activity and A $\beta$  generation provides a novel molecular mechanism for AD-like neurodegeneration in DS patients.

## RESULTS

### SNX27 Expression Reduces A $\beta$ Generation *In Vitro*

To investigate if SNX27 deficiency affects A $\beta$  generation, we found that down-regulation of SNX27 expression by short hairpin RNAs (shRNAs) in HEK293 cells stably over-expressing human APP695 with the Swedish mutations (HEK293swe) markedly increased A $\beta$  generation (Figure 1A). Furthermore, over-expression of a full-length SNX27 but not a PDZ-domain deficient SNX27 (SNX27 PDZ) construct reversed RNAi-induced A $\beta$  enhancement (Figure 1B). Since A $\beta$  peptide is generated through a sequential cleavage of APP by both  $\beta$ -secretase (BACE1) and  $\gamma$ -secretase, we next determined whether SNX27 decreases A $\beta$  levels by modulating BACE1 protein expression, we measured BACE1 protein levels in SNX27-depleted cells (Figure 1A) and found no change in its protein expression. The A $\beta$  precursor APP was also found largely unchanged even though A $\beta$  was markedly increased by SNX27 knockdown. The unchanged amount of APP may be explained by the fact that only a small fraction of APP is subjected to amyloidogenic cleavage leading to A $\beta$  generation. The potential change in the amount of APP was harder to detect in this particular experiment, where APP was over-expressed by an excessive amount.

### SNX27 Expression Decreases $\gamma$ -secretase Activity *In Vitro* and *In Vivo*

A $\beta$  accumulation can also be attributed to an increase in  $\gamma$ -secretase-mediated cleavage. To determine whether SNX27 affects  $\gamma$ -secretase activity, we first measured APP intracellular domain (AICD) generation (a C-terminal APP  $\gamma$ -cleavage product). We found that SNX27 over-expression decreases AICD generation, while knockdown of SNX27 increases AICD generation in HEK293swe cell crude membranes (Figure 2A).

In addition to APP, the Notch receptor has been previously described as a  $\gamma$ -secretase substrate (Kopan and Goate, 2000). We found that Notch intracellular domain (NICD, the  $\gamma$ -cleavage product of Notch) was increased by knockdown of SNX27 in Notch E (the active form of Notch1) expressing HeLa cells (Figure 2B). Moreover, over-expression of full-length SNX27 but not SNX27 PDZ reversed the NICD increase resulting from SNX27 knockdown (Figure 2C). Likewise, amounts of NICD are higher in the liver lysates of *Snx27<sup>+/-</sup>* mice than in *Snx27<sup>+/+</sup>* controls (Figure 2D). These data indicate that SNX27 expression decreases A $\beta$  production through modulating/inhibiting  $\gamma$ -secretase activity.

To determine whether SNX27 decreases A $\beta$  levels by modulating  $\beta$ -secretase or  $\gamma$ -secretase activity, we first performed a fluorescence resonance energy transfer (FRET)-based  $\beta$ -

secretase activity assay and found that both over-expression and knockdown of SNX27 did not affect  $\beta$ -secretase activity (Figure 3A). However, by using a FRET-based  $\gamma$ -secretase activity assay, we found that over-expression of SNX27 reduces  $\gamma$ -secretase activity, whereas knockdown of SNX27 by a shRNA increases  $\gamma$ -secretase activity in HEK293T cells (Figure 3B). In addition,  $\gamma$ -secretase activity is markedly enhanced in the hippocampi of *Snx27<sup>+/-</sup>* mice than in *Snx27<sup>+/+</sup>* controls (Figure 3C).

### SNX27 Modulates $\gamma$ -secretase Complex Stability through Interaction with Presenilin 1

To determine whether SNX27 regulates  $\gamma$ -secretase activity through physical interactions with the  $\gamma$ -secretase complex, we transfected GST-tagged SNX27 into HEK293T cells and assayed for interactions between GST-SNX27 and  $\gamma$ -secretase subunits by GST pulldown assays. We found that SNX27 can interact with PS1 N-terminal fragment (PS1 NTF) but not with Nicastrin (Figures 4A and Figure S1A). In HEK293T cells co-transfected with GFP-SNX27 and GST-PS1 NTF/GST-PS1 C-terminal fragment (PS1 CTF), both GST-tagged PS1 NTF and PS1 CTF co-precipitated with GFP-SNX27 (Figures 4B and Figure S1B). Furthermore, we performed an *in vitro* binding assay to strengthen our pull-down results. Using GST-PS1 NTF and CTF from HEK293T cells immobilized on glutathione sepharose, we assayed interactions with recombinant purified His6-SNX27. The pulldown assays were performed in a stringent detergent buffer (1% Triton X-100) which dissociates  $\gamma$ -secretase complex (Capell et al., 1998; Li et al., 2000) and weak protein-protein interactions. Results from our *in vitro* binding assays indicate that His6-SNX27 binds to both PS1 NTF and CTF physically (Figures 4C and Figure S1C). Moreover, we found that both GST-full length SNX27 and GST-SNX27 PDZ domain associated with PS1 NTF and PS1 CTF. However, GST-SNX27 lacking a PDZ domain (GST-SNX27 PDZ) largely failed to interact with PS1 protein fragments (Figures 4D and Figure S1D). In addition, using an *in silico* prediction method, we found a putative PDZ binding motif in PS1 (PS1 aa464–467 QFYI). However, according to the previous studies, the C-terminal residue is extracellular (Henricson et al., 2005; Laudon et al., 2005; Spasic et al., 2006), suggesting that this residue may be not a bona fide PDZ binding motif. In order to determine whether the interaction between SNX27 and PS1 is a classical interaction of PDZ domain-PDZ binding motif, we performed an *in vitro* binding assay using GST-PS1 CTF and PS1 CTF 464–467 immobilized on glutathione sepharose, and we found that His6-SNX27 binds to both GST-PS1 CTF and PS1 CTF without QFYI motif (PS1 CTF 464–467) (Figure S2). This suggests that PS1 aa464–467 QFYI motif is not required for SNX27 binding. Furthermore, an antibody against the PS1 loop region co-immunoprecipitated with endogenous SNX27 in human brain lysates (Figures 4E and Figure S1E), confirming our pull-down results. These results demonstrate a physical interaction between SNX27 and PS1.

### SNX27 Expression Affects the Integrity of $\gamma$ -secretase Complex

As SNX27 has been found to be a crucial regulator of endocytosis/recycling, we determined whether SNX27 regulates trafficking of the  $\gamma$ -secretase complex. We performed a biotinylation assay and found that over-expression (Figure S3A) or knockdown of SNX27 (Figure S3B) failed to affect cell surface amounts of PS1 NTF, PS1 CTF, Nicastrin and Pen-2. In addition, unlike the effect on recycling of glutamate receptors that we previously

observed (Loo et al., 2014; Wang et al., 2013b), over-expression or knockdown of SNX27 in HEK293T cells did not affect the recycling rate of biotin labeled PS1 (Figure S3C and S3D).

To study the gain-of-function of SNX27 on  $\gamma$ -secretase complex stability and A $\beta$  generation, we used an adeno-associated viral (AAV) vector encoding either enhanced GFP (eGFP) or human SNX27-IRES-eGFP cDNA to over-express eGFP (as control) or SNX27 in primary neurons and mouse brain. Over-expression of human SNX27 in rat primary neurons reduced expression amounts of  $\gamma$ -secretase subunits, including PS1 NTF, PS1 CTF, Pen-2 and Aph-1a (Figure 5A). As expected, SNX27 over-expression up-regulated expression of glutamate receptor subunits GluR1 and NR1 (Figure 5A), supporting the differential effects of SNX27 in regulating trafficking/metabolism of  $\gamma$ -secretase complex and glutamate receptors.

Similar to the result obtained from SNX27 knockdown study in HEK293swe cells (Figure 1A), the protein amounts of  $\gamma$ -secretase subunits were unchanged in the hippocampi of *Snx27<sup>-/-</sup>* compared to that in *Snx27<sup>+/+</sup>* mice, App protein levels were, however, slightly decreased in the hippocampi of *Snx27<sup>-/-</sup>* compared to that in *Snx27<sup>+/+</sup>* mice (Figure S4). This slight reduction in App in *Snx27<sup>-/-</sup>* mouse brain may be due to increased cleavage by  $\gamma$ -cleavage.

To determine whether *Snx27* deletion affects integrity of the  $\gamma$ -secretase complex, we examined  $\gamma$ -secretase complex levels using native PAGE. The amounts of high molecular weight  $\gamma$ -secretase complex were more abundant in the hippocampi of *Snx27<sup>+/-</sup>* compared to that in *Snx27<sup>+/+</sup>* mice (Figure 5B). Those data may suggest that *Snx27* deficiency enhances the integrity of the  $\gamma$ -secretase complex.

### SNX27 Over-expression Decreases A $\beta$ Generation *In Vivo*

An SNX27 over-expression mouse model was developed in which AAV-SNX27 was stereotactically injected into one side of the hippocampus of the Tg2576 mouse, an well-established model exhibiting accelerated A $\beta$  amyloidosis attributable to expression of familial AD Swedish mutations (Hsiao et al., 1996). As the control, AAV-eGFP was stereotactically injected into the opposing hippocampus of the same mouse. Four weeks after stereotactic injection of the virus, the mice were sacrificed and the hippocampi were isolated for A $\beta$  ELISA and immunoblot analysis. Expression of human SNX27 in the hippocampus of Tg2576 mice (AAV-SNX27) resulted in a decrease of both A $\beta$ 40 and A $\beta$ 42 amounts in the hippocampus of Tg2576 mice compared to that in AAV-eGFP infected Tg2576 mice (Figure 6A). In addition, over-expression of human SNX27 in Tg2576 mouse brains by AAV infection increased protein levels of APP CTFs compared to that in AAV-eGFP infected mice (Figure 6B). As expected, over-expression of SNX27 resulted in up-regulation of glutamate receptor subunits GluR1 and GluR2 (Figure 6B).

### Genetic Deletion of *Snx27* Promotes A $\beta$ Generation and Neuronal Loss in a Transgenic Mouse Model of AD

We crossed male Tg2576 mice with female *Snx27<sup>+/-</sup>* mice and examined soluble human A $\beta$  levels in 2-month-old *Tg2576;Snx27<sup>+/+</sup>* and *Tg2576;Snx27<sup>+/-</sup>* mice. Both hA $\beta$ 40 and hA $\beta$ 42



amounts were higher in the hippocampi of *Tg2576;Snx27<sup>+/-</sup>* mice compared to that in *Tg2576;Snx27<sup>+/+</sup>* mice (Figure 6C). NeuN has been previously characterized as a marker of mature neurons in the adult brain, and NeuN staining is lost in degenerating neurons (Larsson et al., 2001; Wyss-Coray et al., 2002). In the absence of the human APP transgene, *Snx27<sup>+/-</sup>* mice did not show loss of NeuN staining compared to *Snx27<sup>+/+</sup>* littermates (Figure S5). However, in *Tg2576;Snx27<sup>+/-</sup>* mice, the dentate gyrus (DG) subregion and the cortical region exhibit a loss of NeuN immunostaining (Figure 7A). The numbers of NeuN-positive neurons in CA1 and CA3 regions showed no significant difference between *Tg2576;Snx27<sup>+/+</sup>* and *Tg2576;Snx27<sup>+/-</sup>* mice (Figure 7A). Taken together, our data show that *Snx27* deficiency increases A $\beta$  levels and A $\beta$ -mediated neuronal loss, supporting a role of *Snx27* in regulating A $\beta$  generation.

## DISCUSSION

Our study investigated a molecular mechanism for  $\gamma$ -secretase regulation by SNX27, a protein trafficking regulator that has been recently demonstrated to play an important role in the pathogenesis of Down syndrome (Loo et al., 2014; Wang et al., 2013b). SNX27 binds to PS1 and disrupts the  $\gamma$ -secretase complex/activity and the consequent cleavage of  $\gamma$ -secretase substrates, including APP and Notch. The mechanism underlying SNX27 regulated A $\beta$  generation is complicated, as it has been reported that SNX27 regulates trafficking of several important transmembrane receptors, such as  $\beta$ 2-adrenergic receptor (Laufer et al., 2010; Temkin et al., 2011), 5HT4a receptors (Joubert et al., 2004) and GIRK channels (Lunn et al., 2007; Munoz and Slesinger, 2014). The contribution of these pathways may also have additional effects in APP processing, as the  $\beta$ 2-adrenergic receptor has been reported to modulate A $\beta$  generation. (Ni et al., 2006). Moreover, it has been reported that SNX27 regulates trafficking of several transmembrane proteins in association with the retromer complex (Steinberg et al., 2013). Two components of retromer complex, VPS26 and VPS35 (Muhammad et al., 2008; Small et al., 2005; Wen et al., 2011), are involved in regulating  $\beta$ -secretase activity and endocytic trafficking of BACE1, hence regulating A $\beta$  generation. However, we found that SNX27 only regulates  $\gamma$ -secretase complex and activity without affecting trafficking and activity of BACE1 (Figure S3A and S3B). In addition, SNX27 has been reported to regulate recycling of glutamate receptors from early endosomes to the plasma membrane. As the SNX27/retromer complex is essential for preventing lysosomal degradation and maintaining surface levels of several transmembrane proteins (Steinberg et al., 2013; Temkin et al., 2011), SNX27 could also function to increase  $\gamma$ -secretase recruitment from early endosomes to plasma membrane. However, we did not detect an SNX27-dependent change in the rate of recycling of  $\gamma$ -secretase subunits (Figure S3C and S3D). Therefore, we favor a model that SNX27 may directly interact with and thus disrupts the integrity of the  $\gamma$ -secretase complex in early endosomes (Figure 7B). Since previous reports indicate that SNX27 binds the APP NPxY peptide sequence through its FERM-like domain (Ghai et al., 2011), it will be very interesting to examine the effects of SNX27 on APP trafficking in the future studies. In our previous study, we found that SNX27 is down-regulated in DS brains through a miR-155-C/EBP $\beta$ -SNX27 pathway. miR-155 is encoded by Chromosome 21, which is only triplicated in DS and not in AD, and we found that the expression of SNX27 in our cohort of sporadic AD

human brains is unchanged. However, this does not discount its importance in AD pathogenesis. There are many factors contributing to AD pathology in DS brains, including microRNAs, BACE1, APP and SNX27. It is difficult to determine the relative contribution from each factor, future research and genetic studies may provide us with clues as to whether any SNX27 variants or abnormal modifications are involved in AD pathogenesis.

SNX27 is best known for its role in trafficking synaptic receptors and other transmembrane proteins. Increased SNX27 expression results in up-regulation of synaptic strength by increasing the rate of glutamate receptor recycling, which is important in both DS and AD. The present study reports that down-regulation of SNX27 increases A $\beta$  generation. Since our previous work observed reduced expression of SNX27 in DS brains (Wang et al., 2013b), SNX27 depletion and consequent up-regulation of A $\beta$  generation could contribute to the amyloid deposition associated with AD-like phenotypes in DS. Our studies determined the association between *Snx27* deletion and A $\beta$  generation *in vitro* and in AD transgenic Tg2576 mice. Notably, A $\beta$  elevation associated with *Snx27* deficiency is particularly evident in younger mice (2–3 month of age), and became much less evident in older mice. Mouse A $\beta$ 40 levels were found to only slightly increase but showed no statistical significance in the hippocampi of *Snx27*<sup>+/-</sup> mice (7 month of age) compared to that in *Snx27*<sup>+/+</sup> mice (data not shown). SNX27 deletion has been reported to affect metabolic activities of non-neuronal cells (Steinberg et al., 2013) which may affect A $\beta$  generation (Katsouri et al., 2011; Wang et al., 2013a) and synaptic activity in neurons (Wang et al., 2013b) which has also been reported to modulate A $\beta$  generation (Cirrito et al., 2005; Kamenetz et al., 2003). Hence, the reduced synaptic activity due to *Snx27* deficiency might in turn contribute to APP cleavage leading to a reduction of A $\beta$  generation in *Snx27* KO mouse models, especially in older ages. This may explain why *Snx27* deletion does not enhance A $\beta$  generation in 7 month old Tg2576 mice. Additionally, the loss of neurons resulting from *Snx27* deficiency and consequent reduction of A $\beta$  generation in aged neurons could neutralize the effect of *Snx27* deficiency-induced A $\beta$  generation in older Tg2576 mice. *Snx27* function in synaptic plasticity-dependent cognitive function and A $\beta$  generation may suggest a fundamental link between cognitive decline and amyloidogenic APP processing that is disrupted in DS/AD.

## EXPERIMENTAL PROCEDURES

### Cells, Antibodies, and Reagents

HEK293 cells and HEK293 cells stably expressing human APP Swedish mutations (HEK293Swe) were cultured in DMEM (Hyclone) supplemented with 10% FBS (Gibco) and 1% penicillin/streptomycin (Gibco), in the absence and presence of 400  $\mu$ g/mL G418 (Sigma), respectively.

Primary cortical neurons from embryonic day 17 (E17) rat pups were maintained in neurobasal medium supplemented with B27 and 0.8mM glutamine.

Antibodies used in these experiments include: NeuN (mouse mAb, Millipore), Nicastrin (mouse mAb, Abcam), Aph-1a (Invitrogen), Pen-2 (Abcam), Cleaved Notch1 (Val1744, Cell signaling), Anti-Notch1 intracellular domain antibody (rabbit pAb, Abcam), FLAG

(mAb, clone M2, Sigma), GluR1 (mAb, Chemicon), GluR2 (pAb, Millipore), NR1 (mAb, BD Biosciences),  $\alpha$ -tubulin (mAb, Sigma),  $\beta$ -actin (mAb, Sigma), Myc (9E10, Santa Cruz Biotechnology), A $\beta$  (6E10, Covance); The rabbit polyclonal antibodies against PS1 loop (Thinakaran et al., 1996) and SNX27 (Balana et al., 2011) were described previously; The mouse monoclonal antibody (clone 3D5) against BACE1 was described previously (Zhao et al., 2007); The rabbit polyclonal antibody 369 against the APP C-terminus (Xu et al., 1997), Anti-Nicastrin (Ru716) and Anti-PS1 NTF antibody (Ab14) was developed in our laboratory.

### Crossing *Snx27*<sup>+/-</sup> Mice with Tg2576 Mice

Female heterozygous *Snx27* knockout (*Snx27*<sup>+/-</sup>) mice (Cai et al., 2011; Wang et al., 2013b) were crossed with male heterozygous Tg2576 mice harboring Swedish familial mutations in human APP gene (Hsiao et al., 1996) to generate *Tg2576;Snx27*<sup>+/+</sup> and *Tg2576;Snx27*<sup>+/-</sup> mice. All procedures involving animals were performed under the guidelines of Sanford-Burnham Medical Research Institute (SBMRI) Institutional Animal Care and Use Committee.

### Constructs

The pCI-neo-SNX27-Myc plasmid and the pCI-neo control plasmids were described previously (Rincon et al., 2007; Wang et al., 2013b). The pIPuro vector was generated from pCDNA3 with an IRES-Puromycin resistance marker cloned into the 3' XbaI site. FLAG was inserted into HindIII/BamHI sites using 5'-agcttaccatggactacaagacgatgacgataaaggagcg and 5'-GATCCGCCTCCTTTATCGTCA TCGTCTTTGTAGTCCATGGTA oligos, where the full-length SNX27 and SNX27 PDZ DNA fragments were cloned in-frame using BamHI and NotI cloning sites. His6-SNX27 construct was generated by inserting full-length human SNX27 into a pTrcHis A vector (Invitrogen). The DNA fragments encoding the PS1 NTF, PS1 CTF, PS1 CTF lacking last 4 amino acids, SNX27 and SNX27 PDZ were inserted into the pRK5mGST vector (Huang et al., 2013) to generate GST-tagged constructs. Notch N E plasmid was previously reported (Schroeter et al., 1998).

### RNA Interference

Targeting sequences of short hairpin RNAs for human SNX27 (shRNA1: CCTGAAGAGAGAGTTTGCC, shRNA2: GGTTACATCAAAGCAGAAG) or scrambled shRNA were constructed into a pSuper construct (Invitrogen) with BglII and SalI enzymatic sites. The human SNX27 siRNA used was: 5'-CCAGAUGGAACAACGGUATT-3'. The control siRNA was purchased from QIAGEN.

### A $\beta$ Immunoblot and ELISA Assay

HEK293s we cells in 6-well plates were transfected with either SNX27-myc/control vector or SNX27 shRNA/scramble RNA. To detect the total level of secreted A $\beta$ , cells were transfected for 24–48h and then incubated with 1ml OPTI-MEM for 4h. Conditioned media was then collected and incubated with trichloroacetic acid (1:9 v/v) overnight at 4°C for



protein precipitation. Precipitated proteins were subjected to Immunoblot with the anti-human A $\beta$  antibody 6E10.

Mouse hippocampi were isolated and lysed in RIPA buffer (supplemented with ROCHE protease inhibitors). The levels of A $\beta$ 40 and A $\beta$ 42 were quantified using ELISA kits (Invitrogen), following the manufacturer's protocols.

### Immunoblot Analysis

Treated cells or brain tissues were lysed in Nonidet P-40 lysis buffer (1% NP40 in phosphate-buffered saline supplemented with a protease inhibitor mixture) or 1 $\times$ RIPA buffer (with a protease inhibitor mixture), respectively. Total protein concentrations in cell lysates or brain homogenates were determined by the BCA method (Pierce, Rockford, IL). 30–50 $\mu$ g protein from cell lysates or tissue homogenates were boiled in a SDS sample buffer prior to being separated on Novex<sup>®</sup> 4–20% Tris-Glycine Protein Gels (Invitrogen). Equal protein amounts of lysate were analyzed and immunoblotted with the antibodies as indicated. Densitometric analyses of immunoblots were performed using NIH Image J software.

### Blue Native PAGE

Homogenize brain tissue in 1  $\times$  Sample Buffer (1% DDM, Invitrogen) for 10 min on ice. Centrifuge the lysate at 20,000  $\times$  g for 30 min at 4 $^{\circ}$ C. Add benzonase (endonuclease): 1U/ $\mu$ L. Add MgCl<sub>2</sub>(2mM) at room temperature for 20 min. Centrifuge the lysate at 20,000  $\times$  g for 30 minutes at 4 $^{\circ}$ C. Determine protein concentration by BCA. Add G250 (0.25%) and run 4–16% native gel (Invitrogen) at 150V. After the Coomassie brilliant blue dye front migrated about 1/3 of the gel, replace dark blue cathode buffer with light blue cathode buffer. The gel was incubated in 0.1% SDS, 192 mm glycine, 25 mm Tris and 20% methanol for 10 min at room temperature and then transferred onto PVDF membranes (Millipore). The blot was de-stained for 1 h in distilled water/methanol/acetic acid (60/30/10) and incubated with the indicated antibodies.

### *In Vitro* AICD Generation Assay

The *in vitro* AICD generation assay was modified from methods described previously (Edbauer et al., 2002). Briefly, HEK293swe cells were resuspended (0.5 ml/6cm dish) in ice-cold hypotonic homogenization buffer (10 mM MOPS pH 7.0, 10 mM KCl, without protease inhibitors) and incubated on ice for 10 min. Following homogenization on ice with a VWR1.5mL pestle, a post nuclear supernatant was prepared by centrifugation at 1000g for 15 min at 4 $^{\circ}$ C. Crude membranes were isolated from the post-nuclear supernatant by centrifugation at 13,000g for 40 min at 4 $^{\circ}$ C. The membranes were then resuspended (50  $\mu$ l/6cm dish) in assay buffer (150 mM sodium citrate pH 6.4, supplemented with the protease inhibitors) and AICD was generated by incubation of samples at 37 $^{\circ}$ C for 2 h in a volume of 25  $\mu$ l/assay. After termination of the assay reactions on ice, samples were separated into pellet and supernatant fractions by ultracentrifugation for 1 h at 100,000g at 4 $^{\circ}$ C. The supernatant and pellet fractions were prepared in a SDS loading buffer and then separated by SDS-PAGE on 4–20% Tris-Glycine gels (Invitrogen) and analyzed by immunoblot with anti-APP C-terminal antibody 369.

### **GST Pull-down Assay**

PS1 NTF and PS1 CTF complementary DNAs, or full-length SNX27 and SNX27 deletion constructs were cloned into the pRK5mGST mammalian expression vector. GST-PS1 NTF/CTF constructs were co-transfected with GFP-SNX27 into HEK293T cells, lysates were generated in cell lysis buffer (20mM Tris-HCl pH 7.5, 0.15M NaCl, 5% glycerol, 10mM MgCl<sub>2</sub>, 1% NP40 with protease inhibitors) and GST proteins were precipitated for 2h at 4°C with glutathione sepharose. GST-SNX27 and SNX27 deletion constructs were transfected into HEK293T cells and lysates were probed with glutathione sepharose. Precipitates were washed three times in lysis buffer and boiled in SDS-PAGE loading buffer. Eluates and lysate inputs were immunoblotted for either GFP or endogenous PS1/ nicastrin subunits.

### ***In Vitro* Protein-Protein Binding Assay**

HEK293T cells were seeded at 70% confluency onto 10cm dishes coated with poly-D lysine, and transfected with pRK5mGST-NTF, CTF and CTF constructs lacking the last 4 amino acids. 16h following transfection, cells were lysed in 1% Triton X-100 buffer, and GST proteins were loaded onto glutathione sepharose with gentle agitation at 4 °C for 1–2h. Beads were washed with 1% Triton X-100 and incubated with 3 µg of recombinant His6-SNX27 protein in standard buffer for 2h with gentle agitation at 4 °C. Beads were washed (generally 3 × 800µl for 20 minutes at 4 °C with gentle agitation), and bound complexes were boiled and analyzed by immunoblot analysis. 1µg of recombinant His6-SNX27 was loaded as input.

### **Co-immunoprecipitation**

Human brain tissue were lysed in NP40 buffer (1% Nonidet P-40 in phosphate buffered saline, supplemented with ROCHE protease inhibitors). Lysates were immunoprecipitated using rabbit IgG and indicated antibodies as well as Trueblot IP beads (eBioscience), followed by immunoblot with indicated antibodies.

### **β-secretase Activity Assay**

A FRET based assay commercial kit was used to assess β-secretase activity (Sigma-Aldrich) according to the manufacturer's instructions.

### **γ-Secretase Fluorogenic Substrate Assay**

We performed the assay as described previously (Farmery et al., 2003; Ni et al., 2006). After centrifugation of cell lysates or tissue homogenates at 13,000g for 15 min, pellets were resuspended and then incubated at 37 °C for 2 h in 50 µl of assay buffer (50 mM Tris-HCl, pH 6.8, 2 mM EDTA, 0.25% CHAPSO) containing 8µM fluorogenic substrates (Calbiochem). Fluorescence was measured using a SpectraMax M5 spectrometer (Molecular Devices) with the excitation wavelength set at 355 nm and the emission wavelength set at 440 nm.

## Immunohistochemistry

*Tg2576;Snx27<sup>+/+</sup>* and *Tg2576;Snx27<sup>+/-</sup>* mice were anesthetized and fixed by cardiac perfusion with 4% PFA. Whole brains were excised and post-fixed in 4% PFA overnight. Tissue blocks were embedded in paraffin and 5 $\mu$ m sections were cut. For immunohistochemistry, deparaffinized sections were incubated in citrate buffer (pH 7.0), treated with 3% H<sub>2</sub>O<sub>2</sub> followed by 3% normal horse serum, and incubated overnight at 4°C with primary antibodies against NeuN (1:100), followed by DAB staining using a DAB Peroxidase Substrate Kit (Vector labs). Immunostained sections were examined and fluorescence images collected using a Zeiss fluorescence microscope with AxioVision software.

## Stereotactic Injection of Adeno-associated Virus

Stereotactic injection was performed as described previously (Wang et al., 2013b). Recombinant human SNX27 and eGFP adeno-associated virus (2 $\mu$ l, titer 3 $\times$ 10<sup>12</sup>) were stereotactically injected into the hippocampus of *Tg2576* mice at the following coordinates: anterior posterior, 1.8; medial lateral,  $\pm$ 1.8; dorsal ventral, 1.8. To confirm region-specific over-expression of SNX27 in mouse brains, 4 weeks after injection mice were anesthetized and sacrificed, whereupon brain tissues were rapidly removed. Hippocampal lysates were prepared by homogenizing tissue in RIPA buffer in the absence of protease inhibitors, for A $\beta$  ELISA or immunoblot analysis.

## Supplementary Material

Refer to Web version on PubMed Central for supplementary material.

## ACKNOWLEDGMENTS

We thank T. Golde and C. Ceballos (University of Florida) for generating AAV, J-Y. Hur and Y-M. Li (Memorial Sloan-Kettering Cancer Center) for technical assistance, B. Ranscht, W.C. Mobley, E.H. Koo, S.A. Lipton and G. Thinakaran for helpful discussion, A. Brzozowska-Precht and L. Lacarra for technical help, P. Slesinger (Mount Sinai School of Medicine) and R. Vassar (Northwestern University) for sharing reagents. This work was supported in part by US National Institutes of Health grants (R01 AG038710, R01 AG021173, R01 NS046673, R01 AG030197 and R01 AG044420 to H.X.) and grants from the Alzheimer's Association (to H.X. and Y.-w.Z.) and the Global Down Syndrome Foundation (DSADIIP-13-283543, to H.X.), the American Health Assistance Foundation (to H.X.), National Natural Science Foundation of China (81202419, 81225008, 81161120496, 91332112, and 91332114), the 973 Prophase Project (2010CB535004 to Y.-w.Z.) and Natural Science Funds for Distinguished Young Scholar of Fujian Province (2009J06022 to Y.-w.Z.). Y.-w.Z. is supported by the Program for New Century Excellent Talents in Universities (NCET), the Fundamental Research Funds for the Central Universities and Fok Ying Tung Education Foundation.

## REFERENCES

- Balana B, Maslennikov I, Kwiatkowski W, Stern KM, Bahima L, Choe S, Slesinger PA. Mechanism underlying selective regulation of G protein-gated inwardly rectifying potassium channels by the psychostimulant-sensitive sorting nexin 27. *Proceedings of the National Academy of Sciences of the United States of America*. 2011; 108:5831–5836. [PubMed: 21422294]
- Bertram L, Lill CM, Tanzi RE. The genetics of Alzheimer disease: back to the future. *Neuron*. 2010; 68:270–281. [PubMed: 20955934]
- Cai D, Netzer WJ, Zhong M, Lin Y, Du G, Frohman M, Foster DA, Sisodia SS, Xu H, Gorelick FS, et al. Presenilin-1 uses phospholipase D1 as a negative regulator of beta-amyloid formation.

- Proceedings of the National Academy of Sciences of the United States of America. 2006; 103:1941–1946. [PubMed: 16449386]
- Cai L, Loo LS, Atlashkin V, Hanson BJ, Hong W. Deficiency of sorting nexin 27 (SNX27) leads to growth retardation and elevated levels of N-methyl-D-aspartate receptor 2C (NR2C). *Molecular and cellular biology*. 2011; 31:1734–1747. [PubMed: 21300787]
- Capell A, Grunberg J, Pesold B, Diehlmann A, Citron M, Nixon R, Beyreuther K, Selkoe DJ, Haass C. The proteolytic fragments of the Alzheimer's disease-associated presenilin-1 form heterodimers and occur as a 100-150-kDa molecular mass complex. *The Journal of biological chemistry*. 1998; 273:3205–3211. [PubMed: 9452432]
- Chen F, Hasegawa H, Schmitt-Ulms G, Kawarai T, Bohm C, Katayama T, Gu Y, Sanjo N, Glista M, Rogava E, et al. TMP21 is a presenilin complex component that modulates gamma-secretase but not epsilon-secretase activity. *Nature*. 2006; 440:1208–1212. [PubMed: 16641999]
- Cirrito JR, Yamada KA, Finn MB, Sloviter RS, Bales KR, May PC, Schoepp DD, Paul SM, Mennerick S, Holtzman DM. Synaptic activity regulates interstitial fluid amyloid-beta levels in vivo. *Neuron*. 2005; 48:913–922. [PubMed: 16364896]
- Cullen PJ. Endosomal sorting and signalling: an emerging role for sorting nexins. *Nature reviews Molecular cell biology*. 2008; 9:574–582.
- De Strooper B, Annaert W. Novel research horizons for presenilins and gamma-secretases in cell biology and disease. *Annual review of cell and developmental biology*. 2010; 26:235–260.
- Edbauer D, Willem M, Lammich S, Steiner H, Haass C. Insulin-degrading enzyme rapidly removes the beta-amyloid precursor protein intracellular domain (AICD). *The Journal of biological chemistry*. 2002; 277:13389–13393. [PubMed: 11809755]
- Farmery MR, Tjernberg LO, Pursglove SE, Bergman A, Winblad B, Naslund J. Partial purification and characterization of gamma-secretase from post-mortem human brain. *The Journal of biological chemistry*. 2003; 278:24277–24284. [PubMed: 12697771]
- Ghai R, Mobli M, Norwood SJ, Bugarcic A, Teasdale RD, King GF, Collins BM. Phox homology band 4.1/ezrin/radixin/moesin-like proteins function as molecular scaffolds that interact with cargo receptors and Ras GTPases. *Proceedings of the National Academy of Sciences of the United States of America*. 2011; 108:7763–7768. [PubMed: 21512128]
- Goutte C, Tsunozaki M, Hale VA, Priess JR. APH-1 is a multipass membrane protein essential for the Notch signaling pathway in *Caenorhabditis elegans* embryos. *Proceedings of the National Academy of Sciences of the United States of America*. 2002; 99:775–779. [PubMed: 11792846]
- Hasegawa H, Sanjo N, Chen F, Gu YJ, Shier C, Petit A, Kawarai T, Katayama T, Schmidt SD, Mathews PM, et al. Both the sequence and length of the C terminus of PEN-2 are critical for intermolecular interactions and function of presenilin complexes. *The Journal of biological chemistry*. 2004; 279:46455–46463. [PubMed: 15322109]
- Henricson A, Kall L, Sonnhammer EL. A novel transmembrane topology of presenilin based on reconciling experimental and computational evidence. *The FEBS journal*. 2005; 272:2727–2733. [PubMed: 15943807]
- Hsiao K, Chapman P, Nilsen S, Eckman C, Harigaya Y, Younkin S, Yang F, Cole G. Correlative memory deficits, A $\beta$  elevation, and amyloid plaques in transgenic mice. *Science*. 1996; 274:99–102. [PubMed: 8810256]
- Huang TY, Michael S, Xu T, Sarkeshik A, Moresco JJ, Yates JR 3rd, Masliah E, Bokoch GM, DerMardirossian C. A novel Rac1 GAP splice variant relays poly-Ub accumulation signals to mediate Rac1 inactivation. *Molecular biology of the cell*. 2013; 24:194–209. [PubMed: 23223568]
- Joubert L, Hanson B, Barthet G, Sebben M, Claeysen S, Hong W, Marin P, Dumuis A, Bockaert J. New sorting nexin (SNX27) and NHERF specifically interact with the 5-HT<sub>4a</sub> receptor splice variant: roles in receptor targeting. *Journal of cell science*. 2004; 117:5367–5379. [PubMed: 15466885]
- Kajii Y, Muraoka S, Hiraoka S, Fujiyama K, Umino A, Nishikawa T. A developmentally regulated and psychostimulant-inducible novel rat gene *mrt1* encoding PDZ-PX proteins isolated in the neocortex. *Molecular psychiatry*. 2003; 8:434–444. [PubMed: 12740601]
- Kamenetz F, Tomita T, Hsieh H, Seabrook G, Borchelt D, Iwatsubo T, Sisodia S, Malinow R. APP processing and synaptic function. *Neuron*. 2003; 37:925–937. [PubMed: 12670422]

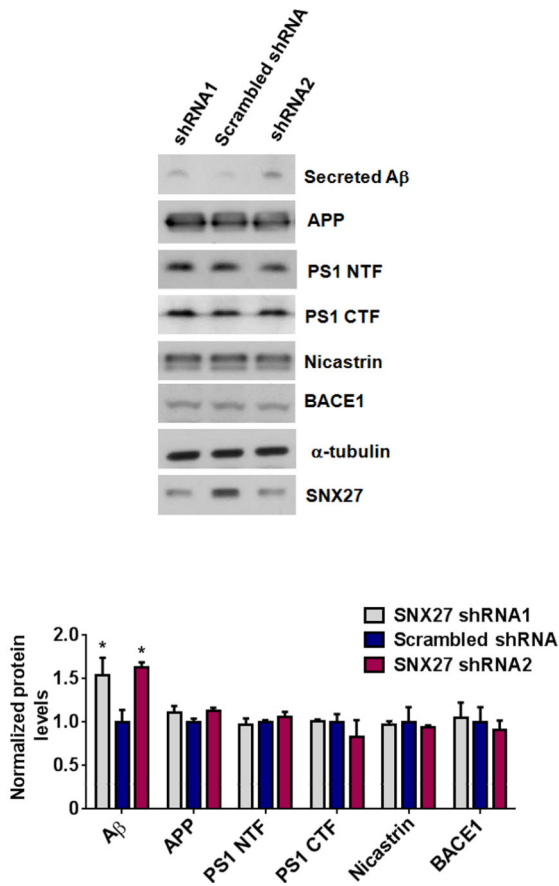
- Katsouri L, Parr C, Bogdanovic N, Willem M, Sastre M. PPARgamma co-activator-1alpha (PGC-1alpha) reduces amyloid-beta generation through a PPARgamma-dependent mechanism. *Journal of Alzheimer's disease : JAD*. 2011; 25:151–162.
- Kimberly WT, LaVoie MJ, Ostaszewski BL, Ye W, Wolfe MS, Selkoe DJ. Gamma-secretase is a membrane protein complex comprised of presenilin, nicastrin, Aph-1, and Pen-2. *Proceedings of the National Academy of Sciences of the United States of America*. 2003; 100:6382–6387. [PubMed: 12740439]
- Kopan R, Goate A. A common enzyme connects notch signaling and Alzheimer's disease. *Genes & development*. 2000; 14:2799–2806. [PubMed: 11090127]
- Larsson E, Lindvall O, Kokaia Z. Stereological assessment of vulnerability of immunocytochemically identified striatal and hippocampal neurons after global cerebral ischemia in rats. *Brain research*. 2001; 913:117–132. [PubMed: 11549375]
- Laudon H, Hansson EM, Melen K, Bergman A, Farmery MR, Winblad B, Lendahl U, von Heijne G, Naslund J. A nine-transmembrane domain topology for presenilin 1. *The Journal of biological chemistry*. 2005; 280:35352–35360. [PubMed: 16046406]
- Lauffer BE, Melero C, Temkin P, Lei C, Hong W, Kortemme T, von Zastrow M. SNX27 mediates PDZ-directed sorting from endosomes to the plasma membrane. *The Journal of cell biology*. 2010; 190:565–574. [PubMed: 20733053]
- Lee J, Retamal C, Cuitino L, Caruano-Yzermans A, Shin JE, van Kerkhof P, Marzolo MP, Bu G. Adaptor protein sorting nexin 17 regulates amyloid precursor protein trafficking and processing in the early endosomes. *The Journal of biological chemistry*. 2008; 283:11501–11508. [PubMed: 18276590]
- Li YM, Xu M, Lai MT, Huang Q, Castro JL, DiMuzio-Mower J, Harrison T, Lellis C, Nadin A, Neduvetil JG, et al. Photoactivated gamma-secretase inhibitors directed to the active site covalently label presenilin 1. *Nature*. 2000; 405:689–694. [PubMed: 10864326]
- Liu X, Zhao X, Zeng X, Bossers K, Swaab DF, Zhao J, Pei G. beta-arrestin1 regulates gamma-secretase complex assembly and modulates amyloid-beta pathology. *Cell research*. 2013; 23:351–365. [PubMed: 23208420]
- Loo LS, Tang N, Al-Haddawi M, Dawe GS, Hong W. A role for sorting nexin 27 in AMPA receptor trafficking. *Nature communications*. 2014; 5:3176.
- Lunn ML, Nassirpour R, Arrabit C, Tan J, McLeod I, Arias CM, Sawchenko PE, Yates JR 3rd, Slesinger PA. A unique sorting nexin regulates trafficking of potassium channels via a PDZ domain interaction. *Nature neuroscience*. 2007; 10:1249–1259.
- Muhammad A, Flores I, Zhang H, Yu R, Staniszewski A, Planel E, Herman M, Ho L, Kreber R, Honig LS, et al. Retromer deficiency observed in Alzheimer's disease causes hippocampal dysfunction, neurodegeneration, and Aβ accumulation. *Proceedings of the National Academy of Sciences of the United States of America*. 2008; 105:7327–7332. [PubMed: 18480253]
- Munoz MB, Slesinger PA. Sorting nexin 27 regulation of g protein-gated inwardly rectifying k(+) channels attenuates in vivo cocaine response. *Neuron*. 2014; 82:659–669. [PubMed: 24811384]
- Ni Y, Zhao X, Bao G, Zou L, Teng L, Wang Z, Song M, Xiong J, Bai Y, Pei G. Activation of beta2-adrenergic receptor stimulates gamma-secretase activity and accelerates amyloid plaque formation. *Nature medicine*. 2006; 12:1390–1396.
- Rincon E, Santos T, Avila-Flores A, Albar JP, Lalioti V, Lei C, Hong W, Merida I. Proteomics identification of sorting nexin 27 as a diacylglycerol kinase zeta-associated protein: new diacylglycerol kinase roles in endocytic recycling. *Molecular & cellular proteomics : MCP*. 2007; 6:1073–1087. [PubMed: 17351151]
- Schobel S, Neumann S, Hertweck M, Dislich B, Kuhn PH, Kremmer E, Seed B, Baumeister R, Haass C, Lichtenthaler SF. A novel sorting nexin modulates endocytic trafficking and alpha-secretase cleavage of the amyloid precursor protein. *The Journal of biological chemistry*. 2008; 283:14257–14268. [PubMed: 18353773]
- Schroeter EH, Kisslinger JA, Kopan R. Notch-1 signalling requires ligand-induced proteolytic release of intracellular domain. *Nature*. 1998; 393:382–386. [PubMed: 9620803]
- Shen J. *Function and Dysfunction of Presenilin*. *Neuro-degenerative diseases*. 2013

- Sherrington R, Rogaev EI, Liang Y, Rogaeva EA, Levesque G, Ikeda M, Chi H, Lin C, Li G, Holman K, et al. Cloning of a gene bearing missense mutations in early-onset familial Alzheimer's disease. *Nature*. 1995; 375:754–760. [PubMed: 7596406]
- Small SA, Kent K, Pierce A, Leung C, Kang MS, Okada H, Honig L, Vonsattel JP, Kim TW. Model-guided microarray implicates the retromer complex in Alzheimer's disease. *Annals of neurology*. 2005; 58:909–919. [PubMed: 16315276]
- Spasic D, Raemaekers T, Dillen K, Declerck I, Baert V, Serneels L, Fullekrug J, Annaert W. Rer1p competes with APH-1 for binding to nicastrin and regulates gamma-secretase complex assembly in the early secretory pathway. *The Journal of cell biology*. 2007; 176:629–640. [PubMed: 17325205]
- Spasic D, Tolia A, Dillen K, Baert V, De Strooper B, Vrijens S, Annaert W. Presenilin-1 maintains a nine-transmembrane topology throughout the secretory pathway. *The Journal of biological chemistry*. 2006; 281:26569–26577. [PubMed: 16846981]
- Steinberg F, Gallon M, Winfield M, Thomas EC, Bell AJ, Heesom KJ, Tavare JM, Cullen PJ. A global analysis of SNX27-retromer assembly and cargo specificity reveals a function in glucose and metal ion transport. *Nature cell biology*. 2013; 15:461–471.
- Temkin P, Lauffer B, Jager S, Cimermancic P, Krogan NJ, von Zastrow M. SNX27 mediates retromer tubule entry and endosome-to-plasma membrane trafficking of signalling receptors. *Nature cell biology*. 2011; 13:715–721.
- Thathiah A, Horre K, Snellinx A, Vandeweyer E, Huang Y, Ciesielska M, De Kloe G, Munck S, De Strooper B. beta-arrestin 2 regulates Abeta generation and gamma-secretase activity in Alzheimer's disease. *Nature medicine*. 2013; 19:43–49.
- Thinakaran G, Borchelt DR, Lee MK, Slunt HH, Spitzer L, Kim G, Ratovitsky T, Davenport F, Nordstedt C, Seeger M, et al. Endoproteolysis of presenilin 1 and accumulation of processed derivatives in vivo. *Neuron*. 1996; 17:181–190. [PubMed: 8755489]
- Wang R, Li JJ, Diao S, Kwak YD, Liu L, Zhi L, Bueler H, Bhat NR, Williams RW, Park EA, et al. Metabolic stress modulates Alzheimer's beta-secretase gene transcription via SIRT1-PPARgamma-PGC-1 in neurons. *Cell metabolism*. 2013a; 17:685–694. [PubMed: 23663737]
- Wang X, Zhao Y, Zhang X, Badie H, Zhou Y, Mu Y, Loo LS, Cai L, Thompson RC, Yang B, et al. Loss of sorting nexin 27 contributes to excitatory synaptic dysfunction by modulating glutamate receptor recycling in Down's syndrome. *Nature medicine*. 2013b; 19:473–480.
- Wen L, Tang FL, Hong Y, Luo SW, Wang CL, He W, Shen C, Jung JU, Xiong F, Lee DH, et al. VPS35 haploinsufficiency increases Alzheimer's disease neuropathology. *The Journal of cell biology*. 2011; 195:765–779. [PubMed: 22105352]
- Wu J, Petralia RS, Kurushima H, Patel H, Jung MY, Volk L, Chowdhury S, Shepherd JD, Dehoff M, Li Y, et al. Arc/Arg3.1 regulates an endosomal pathway essential for activity-dependent beta-amyloid generation. *Cell*. 2011; 147:615–628. [PubMed: 22036569]
- Wyss-Coray T, Yan F, Lin AH, Lambris JD, Alexander JJ, Quigg RJ, Masliah E. Prominent neurodegeneration and increased plaque formation in complement-inhibited Alzheimer's mice. *Proceedings of the National Academy of Sciences of the United States of America*. 2002; 99:10837–10842. [PubMed: 12119423]
- Xu H, Sweeney D, Wang R, Thinakaran G, Lo AC, Sisodia SS, Greengard P, Gandy S. Generation of Alzheimer beta-amyloid protein in the trans-Golgi network in the apparent absence of vesicle formation. *Proceedings of the National Academy of Sciences of the United States of America*. 1997; 94:3748–3752. [PubMed: 9108049]
- Yu G, Nishimura M, Arawaka S, Levitan D, Zhang L, Tandon A, Song YQ, Rogaeva E, Chen F, Kawarai T, et al. Nicastrin modulates presenilin-mediated notch/glp-1 signal transduction and betaAPP processing. *Nature*. 2000; 407:48–54. [PubMed: 10993067]
- Zhao J, Fu Y, Yasvoina M, Shao P, Hitt B, O'Connor T, Logan S, Maus E, Citron M, Berry R, et al. Beta-site amyloid precursor protein cleaving enzyme 1 levels become elevated in neurons around amyloid plaques: implications for Alzheimer's disease pathogenesis. *The Journal of neuroscience : the official journal of the Society for Neuroscience*. 2007; 27:3639–3649. [PubMed: 17409228]
- Zhao Y, Wang Y, Yang J, Wang X, Zhang X, Zhang YW. Sorting nexin 12 interacts with BACE1 and regulates BACE1-mediated APP processing. *Mol Neurodegener*. 2012; 7:30. [PubMed: 22709416]



Zhou S, Zhou H, Walian PJ, Jap BK. CD147 is a regulatory subunit of the gamma-secretase complex in Alzheimer's disease amyloid beta-peptide production. *Proceedings of the National Academy of Sciences of the United States of America*. 2005; 102:7499–7504. [PubMed: 15890777]

A



B

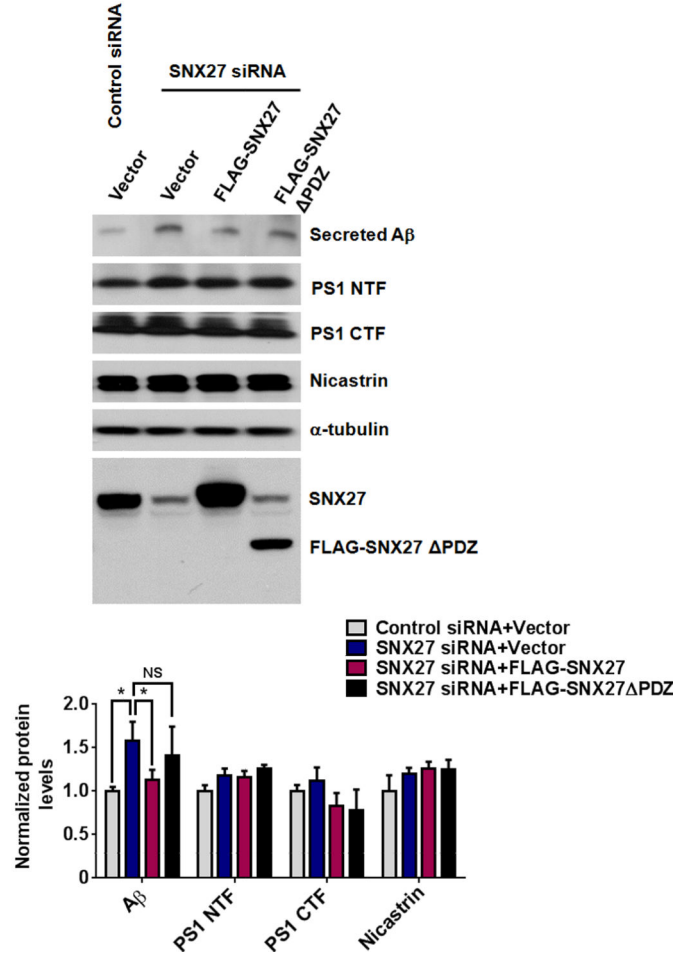


### Figure 1. SNX27 Protein Modulates APP Processing/A $\beta$ Generation

(A) Knockdown of SNX27 using shRNAs in human HEK293swe cells increased secreted A $\beta$ . A $\beta$  in the conditioned medium was precipitated and analyzed by immunoblot analysis. Cell lysates were prepared and 30 $\mu$ g total protein per lane was used for immunoblot analysis,  $\alpha$ -tubulin was used as a loading control.

(B) Knockdown of SNX27 using siRNA in human HEK293swe cells increased secreted A $\beta$ . Over-expression of a full-length SNX27, but not an SNX27 PDZ construct, reversed RNAi-induced A $\beta$  up-regulation. Protein levels were analyzed by immunoblot using antibodies as indicated.

In (A) and (B), data represent mean  $\pm$  SEM,  $n = 3$ ;  $P$  values were calculated using two-tailed Student's  $t$  test; \* $P < 0.05$ , NS: Not Significant.

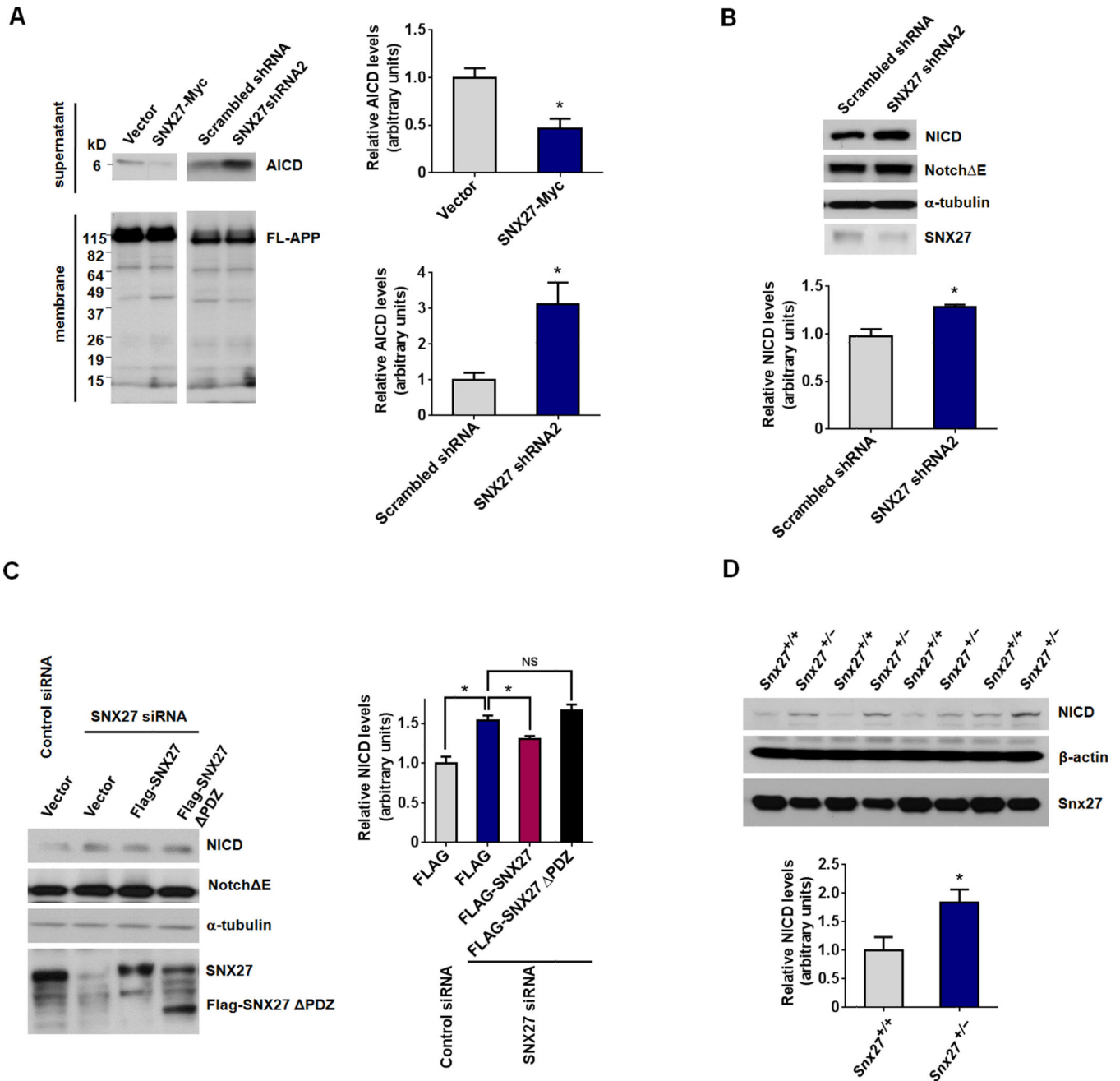


### Figure 2. SNX27 Protein Regulate $\gamma$ -cleavage of APP and Notch

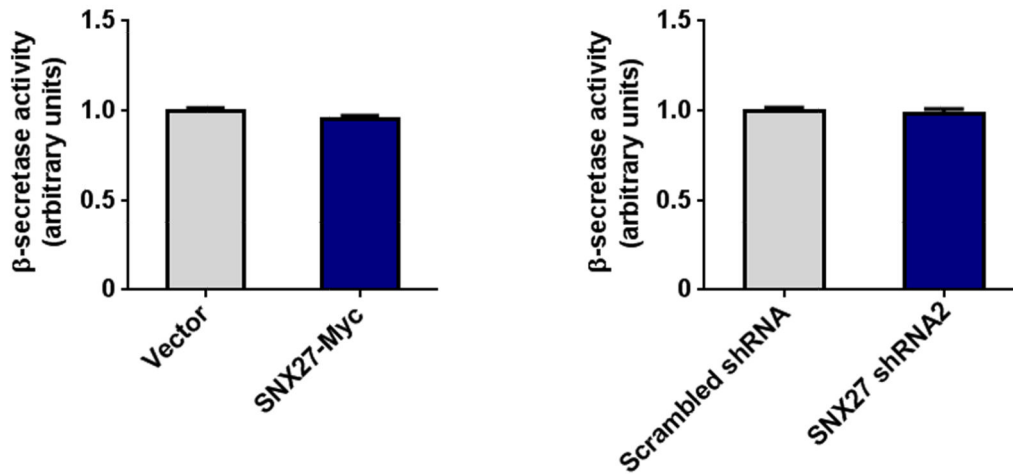
(A) Generation of AICD in crude membrane suspensions from HEK293swe cells transfected with SNX27-Myc/vector control or SNX27 shRNA/scrambled shRNA vector for 48h.

(B) Knockdown of SNX27 using a shRNA increased  $\gamma$ -secretase cleavage of Notch receptors. Expression level of NICD in Notch E expressing HeLa cells transfected with SNX27 shRNA or Scramble shRNA control vectors.

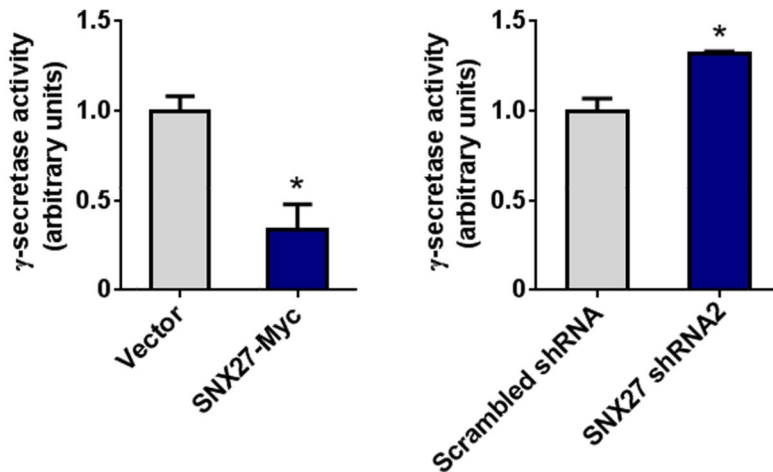
(C) siRNA-mediated knockdown of SNX27 increased NICD generation in Notch E expressing HeLa cells. Over-expression of a full-length SNX27, but not an SNX27 PDZ construct, reversed RNAi-induced NICD enhancement.

(D) Expression levels of NICD in newborn *Snx27<sup>+/+</sup>* and *Snx27<sup>+/-</sup>* mouse liver lysates. Tissue lysates were prepared and 50µg total protein per lane was used for immunoblot analysis, β-actin was used as a loading control. Data represent mean ± SEM,  $n = 3$  for (A) – (C),  $n = 4$  mice for (D); For (A), (B) and (D),  $P$  values were calculated using two-tailed Student's  $t$  test; For (C),  $P$  values were calculated using one-way ANOVA with Tukey's *post hoc* analysis; \* $P < 0.05$ , NS: Not Significant.

A



B



C

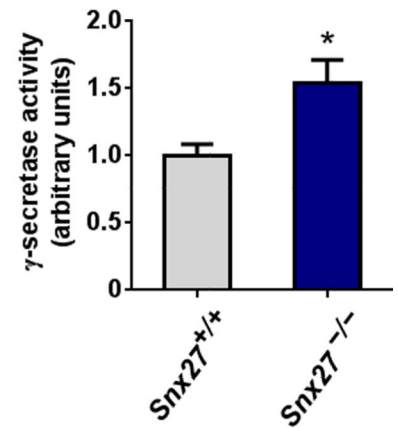


**Figure 3. SNX27 Expression Regulates  $\gamma$ -secretase Activity *In Vitro* and *In Vivo***

(A) Effect of SNX27 modulation on  $\beta$ -secretase activity. Left panel: HEK293swe cells were transfected with SNX27-Myc or control vectors for 48h, and assayed for  $\beta$ -secretase activity as described in Methods.

Right panel: HEK293swe cells were transfected with SNX27 shRNA or Scramble RNA vector for 48h, and assayed for  $\beta$ -secretase activity.

(B) Effect of SNX27 modulation on  $\gamma$ -secretase activity. HEK293swe cells were transfected with SNX27-Myc/control vector or SNX27 shRNA/scrambled shRNA vectors for 48h, and assayed for  $\gamma$ -secretase activity.

(C) Newborn *Snx27*<sup>+/+</sup> and *Snx27*<sup>-/-</sup> mouse tissues were assayed for  $\gamma$ -secretase activity. For (A) – (C), data represent mean  $\pm$  SEM,  $n = 3$ ;  $P$  values were calculated using two-tailed Student's  $t$  test,  $*P < 0.05$ .

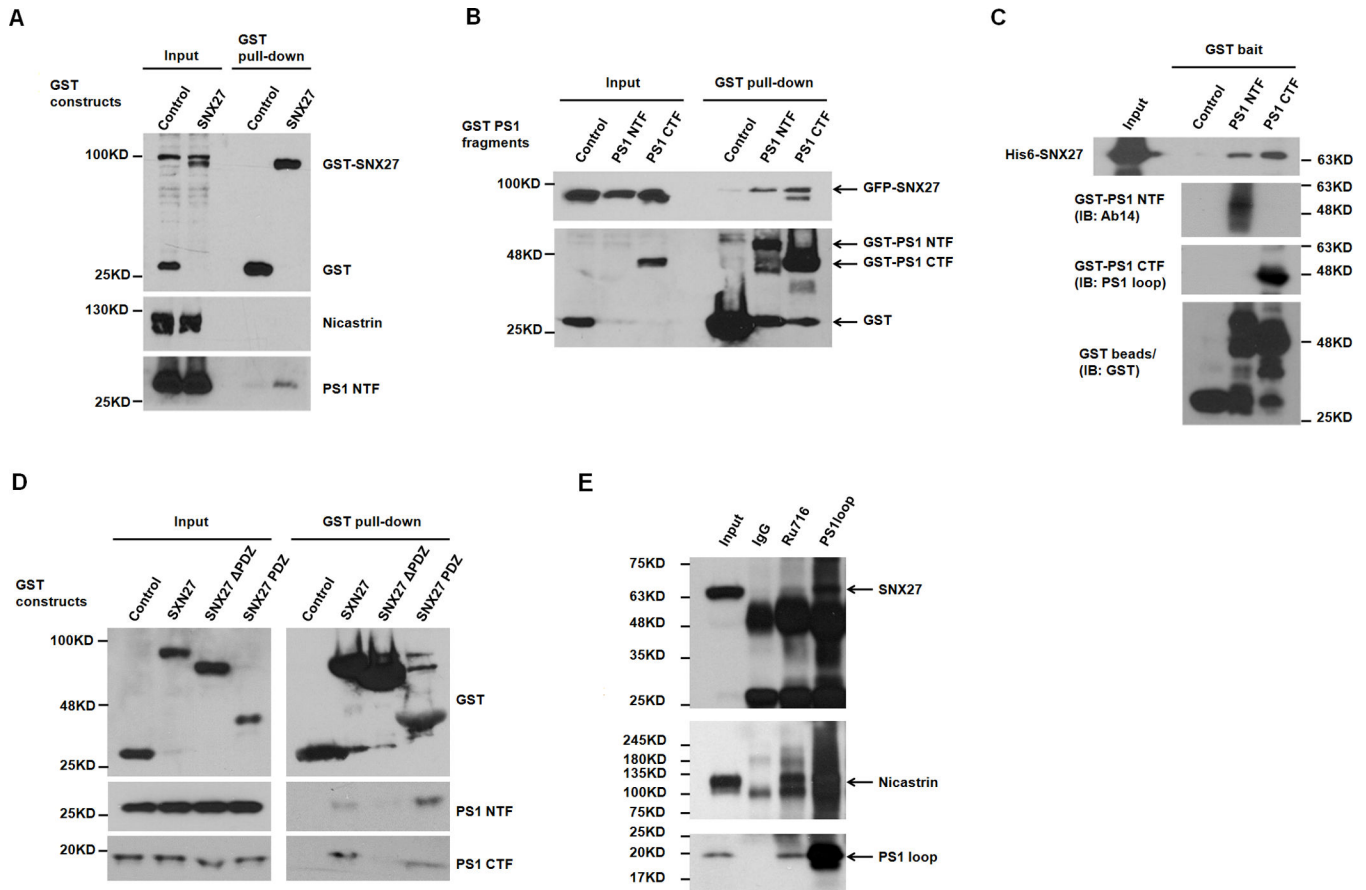


**Figure 4. SNX27 Interacts with the PS1 Subunit of the  $\gamma$ -secretase Complex**

(A) Co-precipitation of the PS1 N-terminal fragment (NTF) with GST-SNX27. HEK293T cells were transfected with either GST-SNX27 or GST control vector. Cell lysates were precipitated with glutathione sepharose beads and immunoblotted with anti-GST, Nicastrin or PS1 NTF antibodies as indicated.

(B) Co-precipitation of SNX27 with PS1 NTF or PS1 CTF fragments. Plasmids expressing GFP-SNX27 were co-transfected with vectors expressing GST alone, GST-NTF or GST-CTF in HEK293T cells. Cell lysates were precipitated with glutathione sepharose beads and immunoblotted for GFP or GST as indicated.

(C) *In vitro* binding of GST-PS1 and His6-SNX27. GST-PS1 NTF and CTF recombinant proteins were purified from GST-PS1 NTF and CTF transfected HEK293T cells and immobilized on glutathione sepharose, and recombinant His6-SNX27 was purified from *E. coli*. The pull-down assay was performed in 1% Triton X-100.

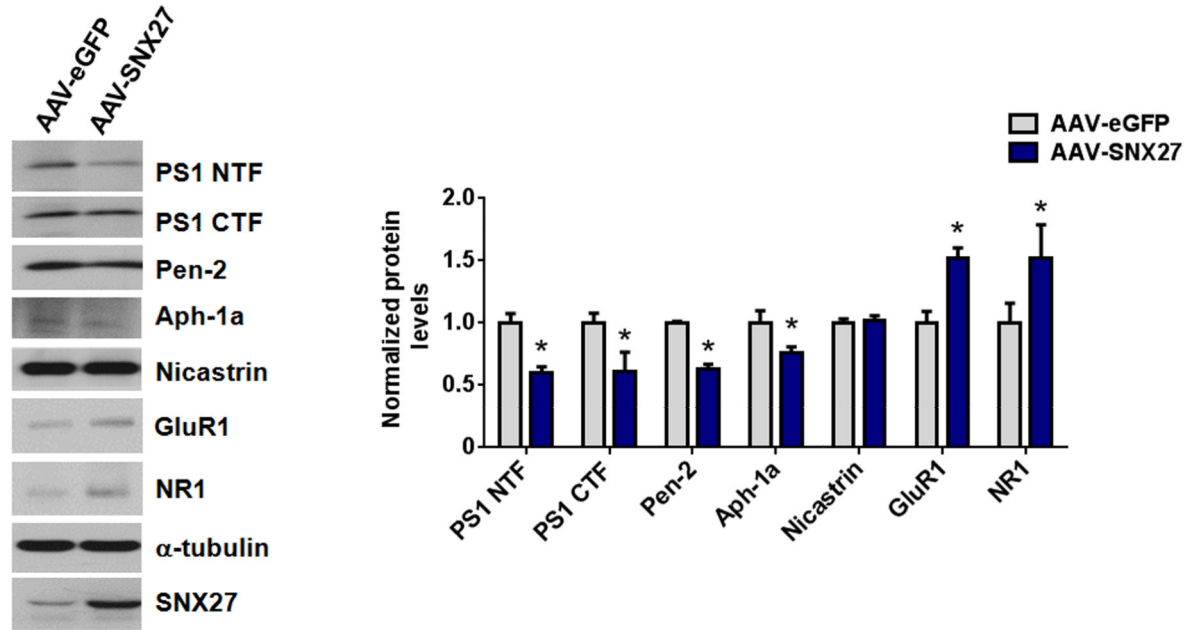
(D) SNX27 PDZ domain is required for interaction between SNX27 and PS1. GST-SNX27, GST-SNX27 lacking the PDZ domain (SNX27  $\Delta$ PDZ) or GST-SNX27 PDZ expressed in HEK293T cells were precipitated with glutathione sepharose beads, and endogenous PS1 NTF and CTF was detected by immunoblot.

(E) Co-immunoprecipitation of endogenous SNX27 and  $\gamma$ -secretase subunits in human cerebral cortical tissue. Human cerebral cortical lysate was immunoprecipitated with antibodies against  $\gamma$ -secretase subunits (Ru716 for Nicastrin, PS1 loop for PS1 CTF) or



rabbit IgG as described in Experimental procedures and immunoblotted for the  $\gamma$ -secretase subunits or SNX27 as indicated.

A



B

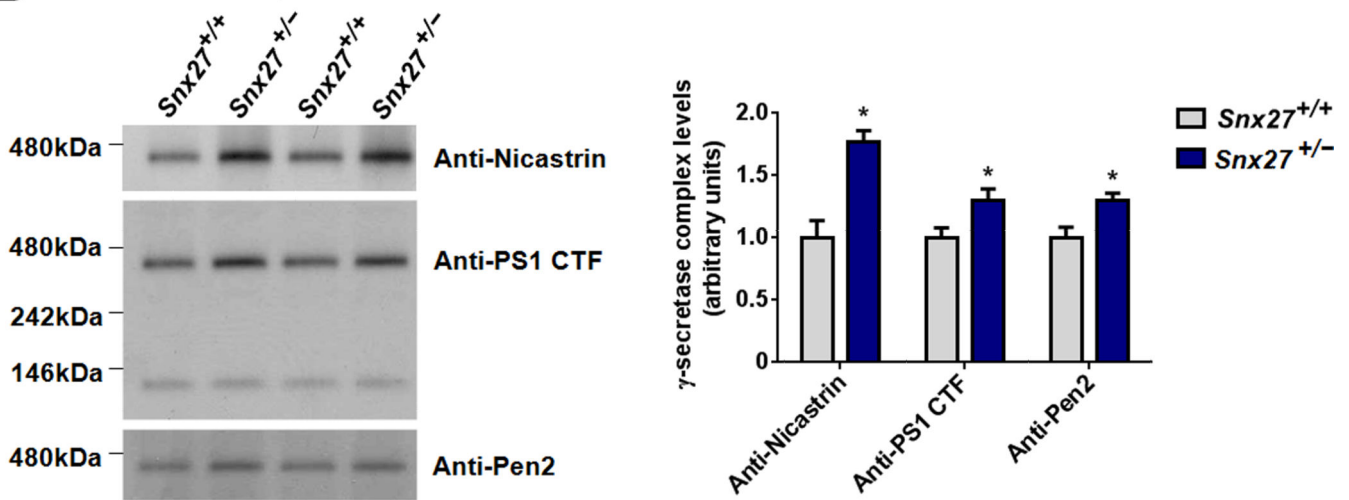


### Figure 5. Modulation of SNX27 Expression Affects $\gamma$ -secretase Complex Stability

(A) Levels of the various  $\gamma$ -secretase subunits (PS1 NTF, PS1 CTF, Pen-2, Aph-1a and Nicastrin) and glutamate receptors (GluR1 and NR1) in rat primary neurons infected with AAV containing SNX27-IRES-eGFP or eGFP (control) were measured by immunoblot. Data represent mean  $\pm$  SEM,  $n = 3$ . P values were calculated using two-tailed Student's t test, \* $P < 0.05$ .

(B) Hippocampi of *Snx27*<sup>+/+</sup> and *Snx27*<sup>+/-</sup> mice were extracted in 1% dodecylmaltoside and processed for Blue Native PAGE analysis. Immunoblot analysis for various  $\gamma$ -secretase subunits indicates that *Snx27* haploinsufficiency in *Snx27*<sup>+/-</sup> mice results in increased levels of mature  $\gamma$ -secretase complex compared to that in wild-type littermates.

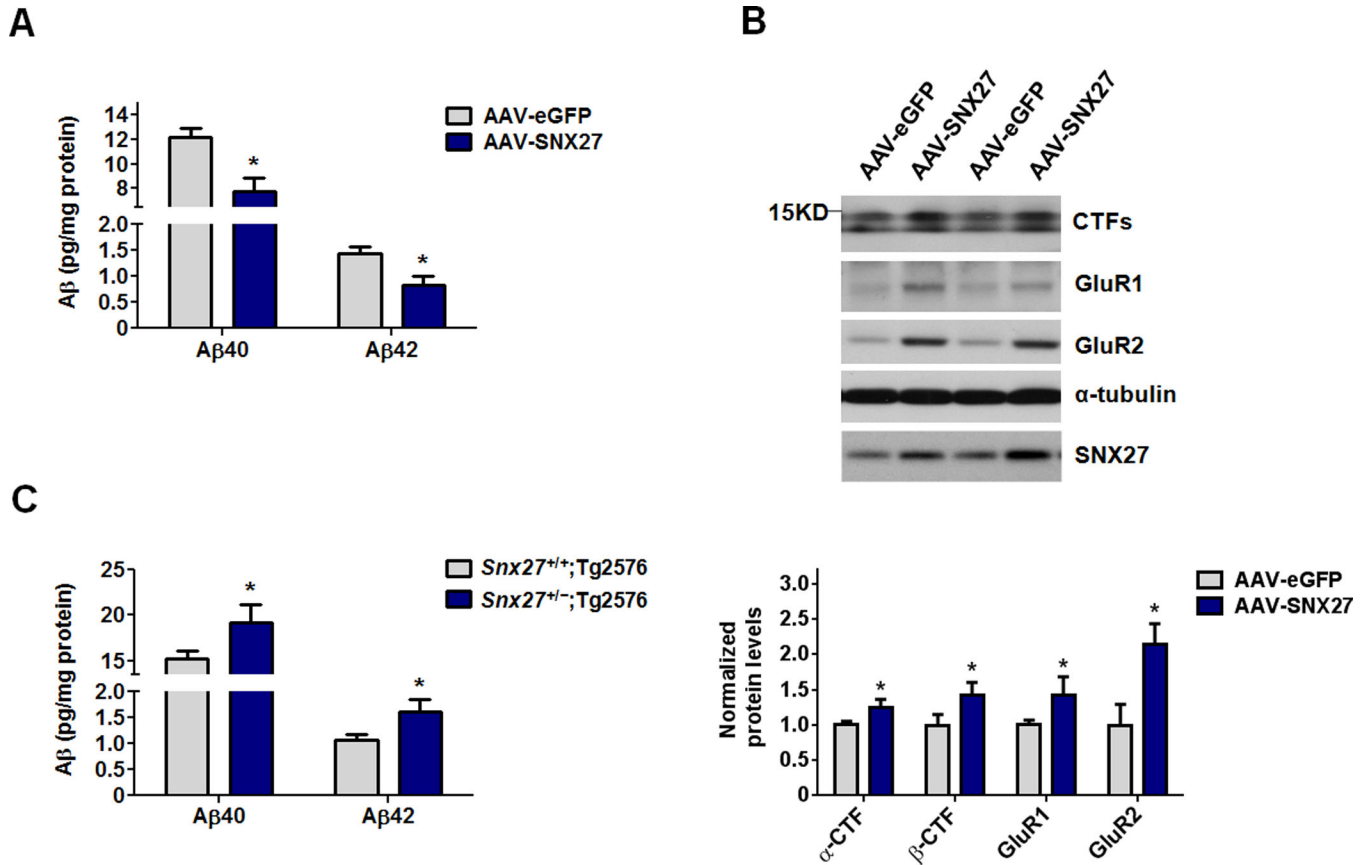


**Figure 6. SNX27 Expression Regulates Aβ Generation in AD Transgenic Mice**

(A) Aβ40 and Aβ42 levels in hippocampal lysates from 6-month old Tg2576 mice injected with AAV-SNX27 (left side) and AAV-eGFP (right side) were individually determined by ELISA. Data represent mean ± SEM, *n* = 3. *P* values were calculated using two-tailed Student's *t* test, \**P* < 0.05.

(B) Immunoblot analysis of APP CTFs, GluR1 and GluR2 levels in hippocampi of Tg2576 mice injected with AAV-eGFP and AAV-SNX27. Signal intensity of the immunoblots was normalized to α-tubulin; *n* = 3. *P* values were calculated using two-tailed Student's *t* test, \**P* < 0.05.

(C) Human Aβ40 and Aβ42 levels were measured by ELISA in hippocampal lysates from 2–3 month old *Snx27*<sup>+/+</sup>;Tg2576 and *Snx27*<sup>+/-</sup>;Tg2576 mice. Data represent mean ± SEM; *Snx27*<sup>+/+</sup>;Tg2576, *n* = 4; *Snx27*<sup>+/-</sup>;Tg2576, *n* = 5. *P* values were calculated using two-tailed Student's *t* test, \**P* < 0.05.

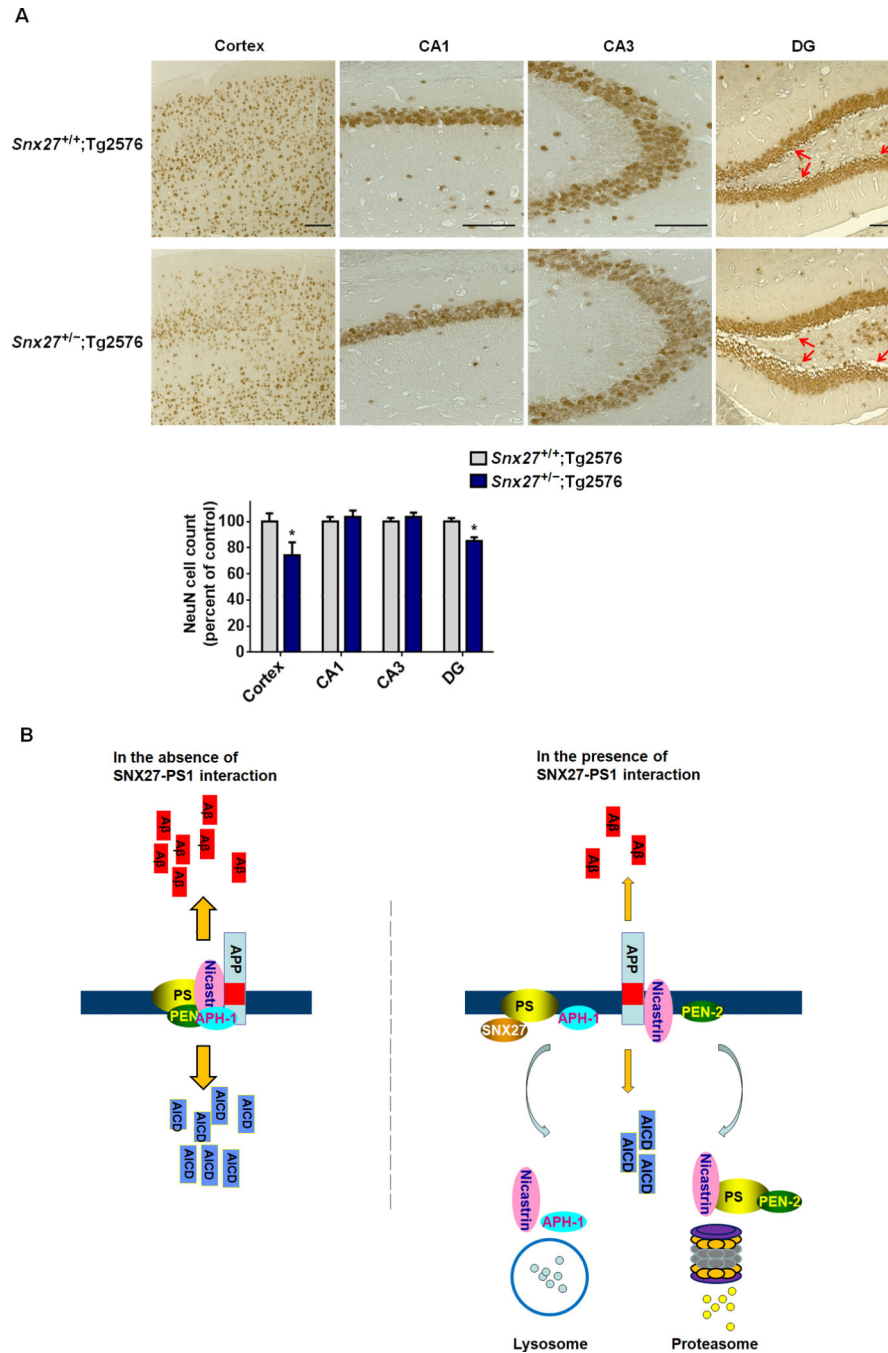


**Figure 7. Genetic Deletion of *Snx27* Promotes Neuronal Loss in AD Transgenic Mice**  
 (A) Neuronal loss in Tg2576 mouse brain with *Snx27* haploinsufficiency. Brain sections from 6-month-old Tg2576 mice with *Snx27*<sup>+/-</sup> or *Snx27*<sup>+/+</sup> backgrounds were analyzed for NeuN immunostaining. *Snx27*<sup>+/-</sup>;Tg2576 brain sections showed a comparatively higher level of neuronal loss in cortical and hippocampal dentate gyrus (DG) but not CA1 and CA3 subregions compared to *Snx27*<sup>+/+</sup>;Tg2576 mice as determined by NeuN staining. Data represent mean ± SEM, *Snx27*<sup>+/+</sup>;Tg2576, *n* = 3; *Snx27*<sup>+/-</sup>;Tg2576, *n* = 3. *P* values were calculated using two-tailed Student's *t* test, \**P* < 0.05. Scale bar = 100μm.

(B) A schematic model of SNX27 in regulating  $\gamma$ -secretase complex formation and A $\beta$  generation. SNX27 binds to PS1 and disassociates the  $\gamma$ -secretase complex whose individual components are degraded by lysosomes and/or proteasomes, thereby reducing APP  $\gamma$ -cleavage. As SNX27 is down-regulated in Down syndrome brains, reduced SNX27 levels may also contribute to amyloid pathology in Down syndrome.